Development 129, 3645-3656 (2002)
Printed in Great Britain © The Company of Biologists Limited 2002
DEV5036

Drumstick is a zinc finger protein that antagonizes Lines to control patterning and morphogenesis of the *Drosophila* hindgut

Ryan B. Green[1], Victor Hatini[2], Katherine A. Johansen[3], Xue-Jun Liu[3,*] and Judith A. Lengyel[1,3,†]

[1]Molecular Biology Institute, [3]Department of Molecular, Cell and Developmental Biology, UCLA, Los Angeles, CA 90095-1606, USA
[2]Department of Cell and Developmental Biology, University of Pennsylvania, School of Medicine, 1223 BRB2, 421 Curie Boulevard, Philadelphia, PA 19104-6058, USA
*Present address: The R. W. Johnson Pharmaceutical Research Institute, La Jolla, CA, USA
†Author for correspondence (e-mail: jlengyel@ucla.edu)

Accepted 15 May 2002

SUMMARY

Elongation of the *Drosophila* embryonic hindgut epithelium occurs by a process of oriented cell rearrangement requiring the genes *drumstick* (*drm*) and *lines* (*lin*). The elongating hindgut becomes subdivided into domains – small intestine, large intestine and rectum – each characterized by a specific pattern of gene expression dependent upon normal *drm* and *lin* function. We show that *drm* encodes an 81 amino acid (10 kDa) zinc finger protein that is a member of the Odd-skipped family. *drm* expression is localized to the developing midgut-hindgut junction and is required to establish the small intestine, while *lin* is broadly expressed throughout the gut primordium and represses small intestine fate. *lin* is epistatic to *drm*, suggesting a model in which localized expression of *drm* blocks *lin* activity, thereby allowing small intestine fate to be established. Further supporting this model, ectopic expression of Drm throughout the hindgut produces a *lin* phenotype. Biochemical and genetic data indicate that the first conserved zinc finger of Drm is essential for its function. We have thus defined a pathway in which a spatially localized zinc finger protein antagonizes a globally expressed protein, thereby leading to specification of a domain (the small intestine) necessary for oriented cell rearrangement.

Key words: *Drosophila melanogaster*, Hindgut, Cell rearrangement, Patterning, Zinc finger, Relief of repression

INTRODUCTION

Cell rearrangement drives many morphogenetic processes. During vertebrate gastrulation, non-epithelial mesodermal cells intercalate and converge toward the midline in a process designated convergent extension, resulting in dramatic elongation of the embryonic axis (Warga and Kimmel, 1990; Keller et al., 1985). Rearrangement of non-epithelial cells also occurs during invertebrate development, including the formation of *Drosophila* ovarian terminal filaments and the migration of ovarian border cells (Godt and Laski, 1995; Montell, 1999).

Cells can also rearrange while remaining constrained within an epithelial sheet. This type of rearrangement is responsible for elongation of both the *Drosophila* germ band and the *C. elegans* dorsal epidermis (Irvine and Wieschaus, 1994; Heid et al., 2001). Similarly, epithelial cell rearrangement causes elongation of developing tubes, including the sea urchin archenteron, *C. elegans* intestine, and *Drosophila* posterior spiracles (Ettensohn, 1985; Leung et al., 1999; Brown and Castelli-Gair Hombría, 2000).

For a field of epithelial cells to change shape in a coherent and directed manner, cell rearrangement within the epithelium must be oriented. In the case of the elongating *Drosophila* germ band, this orientation depends on the patterning of the anteroposterior axis of the embryo (Irvine and Wieschaus, 1994). Later, however, during development of epithelial organs, cell rearrangement is oriented to newly established axes that are specific to the organ itself. Examples include the elongation of the insect Malpighian tubule relative to signals from the tip cell, epithelial migration during tracheal system development relative to localized FGF signals in surrounding mesoderm, and eversion of the leg imaginal disc in response to segmentally localized Notch signaling (Skaer, 1993; Bradley and Andrew, 2001; Rauskolb and Irvine, 1999). A central problem in epithelial morphogenesis, therefore, is to understand how the positional cues (i.e. spatial patterning) that orient cell rearrangement are established.

The *Drosophila* hindgut provides a model system in which to investigate patterning and its role in orienting cell rearrangement. The embryonic hindgut is a single-layered epithelium that elongates by both cell rearrangement and cell shape change (Skaer, 1993; Lengyel and Liu, 1998; Iwaki et al., 2001). Genes controlling each step of the morphogenetic process (specification and internalization of the primordium, maintenance and elongation, and specification and patterning

of subdomains) have been identified (Lengyel and Iwaki, 2002). In particular, the genes *drumstick* (*drm*) and *lines* (*lin*) are required for both patterning in the prospective small intestine and for the cell rearrangement that drives elongation of the hindgut epithelium. While *drm* is required to commit cells to the small intestine fate, *lin* represses this fate (Iwaki et al., 2001).

By analysis of single and double mutants, we show here that *drm* and *lin* interact genetically, and that *lin* is epistatic to *drm*. The *lin* gene encodes a novel, globally expressed protein that is thought to be a transcriptional regulator (Hatini et al., 2000). We show here that *drm* encodes a small, zinc finger protein expressed in a dynamic, spatially localized pattern that is consistent with the *drm* mutant phenotype. Ectopic expression and biochemical interaction studies indicate that Drm antagonizes Lin activity, probably through direct binding. Thus, a relief-of-repression mechanism allows expression of genes that define the small intestine. The specification of this domain is essential for the oriented cell rearrangement that elongates the hindgut.

MATERIALS AND METHODS

Fly stocks

Previously described mutant alleles used were: drm^{1} (Liu et al., 1999), lin^{2} (Hatini et al., 2000), $Df(2L)tim^{02}$ (Myers et al., 1995), and $Df(2L)ed^{1}$ (Reuter and Szidonya, 1983). The strong UAS-*lin* 8 (used here) and other weaker UAS-*lin* stocks (Hatini et al., 2000), the *byn*-GAL4 hindgut-specific driver (Iwaki and Lengyel, 2002), and the *14-3fkh*-GAL4 driver (Fuss and Hoch, 1998) have been previously described. The drm^{P1} lin^{2} double mutant was generated by recombination. UAS-*lacZ* is from the Bloomington Stock Center (Indiana University, Bloomington, IN).

Generation of *drm* alleles

$Df(2L)drm^{P1}$ and $Df(2L)drm^{P2}$ were generated by mobilization of the *l(2)k10101* P element (Török et al., 1993). New point mutations in *drm* were generated by ethyl methanesulfonate mutagenesis (Grigliatti, 1986). Briefly, mutagenized *cn bw sp* males were crossed to *Gla*/*SM6b* females; 17,757 F_1 progeny chromosomes were tested for failure to complement either $Df(2L)drm^{P1}$ or $Df(2L)drm^{P2}$. To minimize the effects of second site mutations, newly isolated *drm* chromosomes were recombined with ast^{1} $dpp^{d\text{-}ho}$ ed^{1} dp^{ov1} cl^{1} and screened for cross-over events between *ed* (24D3) and *dp* (25A), thus replacing ~80% of the mutagenized chromosome. To identify altered nucleotides, new *drm* chromosomes were balanced over *CyO-GFP* (Casso et al., 2000) for selection and sequencing of homozygous genomic DNA. The three exons were amplified individually by PCR (performed in triplicate), subcloned into pCR2.1 (Invitrogen), sequenced in both directions, and compared to the *cn bw sp* parent chromosome.

Phenotypic analysis

Antibody staining was performed according to standard protocols (Ashburner, 1989) using the following antibodies: anti-Crumbs (Crb, 1:100; labels the apical surface of ectodermally derived tissues including the hindgut) (Tepass et al., 1990) and anti-En (1:5) were obtained from the Developmental Studies Hybridoma Bank at The University of Iowa, Department of Biological Sciences (Iowa City, IA); anti β-gal (1:1000; Promega). In situ hybridization to whole-mount embryos was performed as previously described (Tautz and Pfeifle, 1989) using digoxigenin-labeled RNA probes (Roche Molecular Biochemicals). To avoid cross-reactivity with other members of the *odd* family, a 'zinc-fingerless' *drm*-specific probe was synthesized from a PCR-amplified fragment of the *drm* cDNA 3′UTR. The upstream and downstream primer sequences were 5′-CAAAACTCAGCAAACAACTA-3′ and 5′-GAGTGTGTGTGTAT-GTGTGT-3′, respectively. The specificity of this probe was confirmed by its inability to hybridize to embryos homozygous for the drm^{P1} deficiency (which deletes *drm*, but not *sob*, *odd*, or *bowl*). Other probes were made from cDNA templates of *lin* (Hatini et al., 2000), *upd* (Harrison et al., 1998) (also known as *outstretched*, *os* – FlyBase) and *hh* (Lee et al., 1992). For transverse sections, embryos were labeled with anti-Crb prior to mounting in Epon. Two μm serial sections were cut and stained with 0.01% Toluidine Blue, 0.025% Methylene Blue, 0.025% sodium tetraborate. Whole-mount embryos were analyzed with a Zeiss (Thornwood, NY) Axiophot microscope using differential interference contrast optics. Sections were analyzed by phase contrast microscopy. Images were acquired with a Sony DKC-5000 digital camera and embryos were staged based on morphology (Campos-Ortega and Hartenstein, 1997). Larval feeding assays were performed as described previously (Pankratz and Hoch, 1995).

Molecular manipulations

Standard techniques were used for molecularly characterizing the *drm* gene (Sambrook et al., 1989). The breakpoints of the drm^{P1} and drm^{P2} deletions were determined by plasmid rescue (3′ end) and inverse PCR (5′ end) from the residual P element. The drm^{1} I element insertion was localized by Southern blot and molecularly mapped by inverse PCR. Total RNA for northern blot was isolated from 0- to 17-hour embryos using TRIzol (Invitrogen), and poly(A) RNA isolated by PolyATtract (Promega). Probes were constructed by radiolabeling *Bam*HI fragments of DS01379 P1 phage clone (Kimmerly et al., 1996) for Southern blot, or LD26791 EST clone (Research Genetics) for northern blot. The *drm*-specific primers used for 5′ and 3′ RACE were 5′-GATATTGCGTGCTGTTGTTGGTGCT-3′ and 5′-CTTAAA-CGCCGGGCACCAGTACACA-3′, respectively. Amplification was performed on RACE-adapted cDNA from 0 to 4-hour embryos using the Marathon cDNA Amplification Kit (Clontech).

To make constructs for GAL4:UAS expression, the following oligonucleotides were used:

(a) 5′-CAGTAGATCTCAGTACACATACCGCCTGTCAA-3′,
(b) 5′-GTCAGAATTCAAGATGCGTCCGAAGTGCGAGTT-3′,
(c) 5′- GTCAGAATTCATGTTTGCTGTAATGCGAAT-3′,
(d) 5′-CTGAGGTACCACAACGGGGTTTTACGCTTGATA-3′,
(e) 5′-CTGACTCGAGATATGTTTATGTGGTATTTAAG-3′,
(f) 5′-GACTCTCGAGTTACTCGCACTTCGGACGCATCTTG-3′,
(g) 5′-CTGAAGATCTGCGAAGGAAATGTTACTGA-3′,
(h) 5′-CCTGATGATCCACGAGTGCACCCACAAGTCC-3′,
(i) 5′-CCTGAGATCACCTATTCGGGCGAGGTGTGCGGC-3′.

The various *drm* domains (see Fig. 6) were amplified from either *cn bw sp* cDNA or the LD26791 EST clone using the following restriction site-modified oligo pairs (cut sites underlined above): Drm (a and e); C-Drm (b and e); N-Drm (c and f). Amplified products were digested and subcloned into either *Bgl*II/*Xho*I-digested (for Drm) or *Eco*RI/*Xho*I-digested pUAST (Brand and Perrimon, 1993). Point mutations were created by site-directed mutagenesis with the QuikChange XL Kit (Stratagene) using the following oligonucleotides and their complements (altered nucleotides underlined above): R46C (h) and C57G (i). HA-tagged derivatives of each construct were made by incorporating the HA epitope sequence, in frame, into the PCR primers. A UAS-DrmEST construct expressing the full-length *drm* cDNA was also generated by subcloning the 2.1 kb *Xho*I fragment from LD26791 into pUAST. The gain-of-function phenotypes of UAS-Drm and UAS-DrmEST were indistinguishable (data not shown). The *drm* genomic DNA rescue construct was generated by subcloning the 18.1 kb *Sgr*A1 (blunt-ended)/*Not*I fragment from DS01379 into *Not*I/*Hpa*I-digested pCaSpeR-4 (Thummel and Pirrotta, 1992). The *drm*-GAL4 construct was generated by

amplifying 7.1 kb of the *drm* promoter (primers d and g, cut sites underlined above), digesting with *Kpn*I and *Bgl*II, and subcloning upstream of GAL4 in *Kpn*I/*Bam*HI-digested pGaTB (Brand and Perrimon, 1993). The 10.3 kb *Kpn*I/*Not*I *drm*-GAL4 fragment was then subcloned into pCaSpeR-4.

Germline transformation

Transformation was performed using standard techniques (Ashburner, 1989). Briefly, constructs were coprecipitated at a 2:1 ratio with the pP{Delta2-3} transposase plasmid (Laski et al., 1986), resuspended overnight at 4°C in injection buffer (5 mM KCl, 0.1 mM sodium phosphate, pH 7.8), and filtered through a 0.2 μm cellulose acetate Spin-X column (CoStar) before loading into needles pulled from 1 mm Kwik-Fil borosilicate glass capillaries (World Precision Instruments). DNA was injected using a Transjector microinjector (Eppendorf) into w^{1118} embryos under 80% ethanol.

Coimmunoprecipitation and western blotting

Schneider S2 cells were plated in 6 cm culture dishes 24 hours prior to calcium phosphate transfection with 2.5 μg UAS-Myc-Lin, 2.5 μg UAS-HA-Drm (or Drm derivatives), and 3 μg ubiquitin-GAL4 in 600 μl volume. Transfectant was removed after 12 hours, and cells were harvested 48 hours later. Individual plates of cells were lysed in 400 μl NET buffer (50 mM Tris pH 7.5, 400 mM NaCl, 5 mM EDTA, 1% NP-40, 50 μg/ml phenylmethylsulfonyl fluoride, 1 μg/ml leupeptin, 1.4 μg/ml pepstatin) for 30 minutes and incubated with mouse anti-HA (1:40; monoclonal HA.11 clone 16B12, Covance). Antibody-antigen complexes were collected with Protein G Sepharose (Invitrogen), washed, and resuspended in 100 μl 2× Laemmli buffer. Ten microliters of each sample was separated by SDS-PAGE and transferred to a PVDF membrane. Lin protein was detected using rabbit anti-Myc primary antibody (1:1000; polyclonal c-Myc A-14; Santa Cruz Biotechnology) and HRP-conjugated anti-rabbit secondary antibody (1:3000; Vector Laboratory). Proteins were visualized by ECL Plus detection (Amersham Pharmacia Biotech).

RESULTS

lin is epistatic to *drm*

In both *drm* and *lin* embryos, the hindgut is wider and shorter than that of wild-type embryos (Fig. 1A-C) (Iwaki et al., 2001). Beyond this superficial similarity, however, *drm* and *lin* hindguts are quite distinct. The *drm* hindgut is smaller in diameter, and its epithelium consists of an undulating layer of columnar cells resembling those of the immature wild-type hindgut primordium (Fig. 1F). In contrast, the *lin* hindgut appears distended, consisting of a uniform layer of cuboidal cells similar in appearance to those of the wild-type small intestine (Fig. 1G). The strongly Crb-stained boundary cells, which form two parallel rows running the length of the large intestine, are duplicated in *drm* but are absent in *lin* hindguts (Fig. 1E-G) (Iwaki et al., 2001).

As revealed by gene expression studies, *drm* and *lin* hindguts are improperly patterned, with opposite effects on specification of the large and small intestine. Expression in the dorsal large intestine of *engrailed* (*en*) is retained in *drm* but absent from *lin* hindguts (Fig. 1I-K). Expression in the small intestine of *unpaired* (*upd*), encoding a ligand for the JAK-STAT pathway) is missing from *drm* but greatly expanded in *lin* hindguts (Fig. 1M-O). Similarly, expression in the small intestine of *hedgehog* (*hh*) is reduced in *drm* but greatly expanded in *lin* hindguts (Fig. 1Q-S). These data indicate that, in *drm* embryos, the large intestine is present and the small intestine is greatly reduced or absent; in *lin* embryos, in contrast, the small intestine is greatly expanded and the large intestine is missing.

Because their phenotypes are opposite and easily distinguishable, we used epistasis analysis to ask whether *drm* and *lin* interact genetically. By all criteria applied, the hindgut of the *drm lin* double mutant is remarkably like that of the *lin* single mutant. As in *lin* embryos, the *drm lin* hindgut is short and distended (Fig. 1D), consists of cuboidal epithelial cells, and lacks boundary cell rows (Fig. 1H). Similarly, *en* expression is absent, and both *upd* and *hh* expression are expanded posteriorly (Fig. 1L,P,T). All of these observations taken together show that *lin* is epistatic to *drm* in the hindgut.

Since similarities exist in the genetic regulation of foregut and hindgut development (Pankratz and Hoch, 1995), we asked whether *lin* is also epistatic to *drm* in the foregut. In *drm* embryos, the proventriculus (a multi-layered valve-like structure at the foregut-midgut junction that forms by epithelial folding) does not form, and the foregut is long and narrow (Fig. 1V) (Liu et al., 1999). In both *lin* and *drm lin* embryos, the proventriculus also fails to form, but the foregut is short and wide (Fig. 1W,X). We conclude that *lin* is epistatic to *drm* in the foregut as well.

The gene expression and phenotypic data presented here and previously (Iwaki et al., 2001) demonstrate that *lin* represses and *drm* promotes the small intestine fate. Taken together with the epistasis of *lin* to *drm*, this indicates that *drm* specifies small intestine by antagonizing the repressive effect of *lin*. To understand the molecular basis for this relief of repression, we have molecularly characterized the *drm* gene and analyzed the interaction, both in vivo and in vitro, between Drm and Lin.

drm encodes a small zinc finger protein related to *odd-skipped*

The drm^{1} allele was originally identified as a spontaneously occurring lethal mutation mapping between 23F6 and 24A2 (Liu et al., 1999). *drm* was mapped more precisely by using P element mobilization to generate two overlapping deletions, drm^{P1} and drm^{P2} (Fig. 2A and Table 1). The left and right breakpoints of these deletions were defined molecularly (see Materials and Methods), thereby localizing *drm* to a ~60 kb interval between *tim* and *sob*. Southern blot analysis of drm^{1} genomic DNA revealed an insertion within the 11.9 kb *Bam*HI fragment, characterized by inverse PCR as an I element upstream of the predicted gene CG10016 (Rubin et al., 2000b). Three expressed sequence tag (EST) clones from this gene have been identified (Rubin et al., 2000a); the longest, LD26791, is 2.3 kb and contains three exons (Fig. 2B).

Surprisingly, the LD26791 EST contains only one small open reading frame (ORF) with two zinc finger motifs (Fig. 2D). To address the possibility that larger proteins might arise from this gene by alternative splicing, we characterized CG10016 transcripts by several approaches. A northern blot of embryonic RNA with probes from LD26791 identifies a single 2.5 kb transcript, similar in length to the EST clones (Fig. 2C). RT-PCR with intron-spanning primers failed to identify any splice variants (data not shown). An alternative first exon was identified in a small fraction (~10%) of 5′ RACE products, and several alternative poly(A) addition sites were identified by 3′ RACE; none of these variants affects the ORF length. Sequence of all EST clones, RT-PCR products, 5′ and 3′ RACE

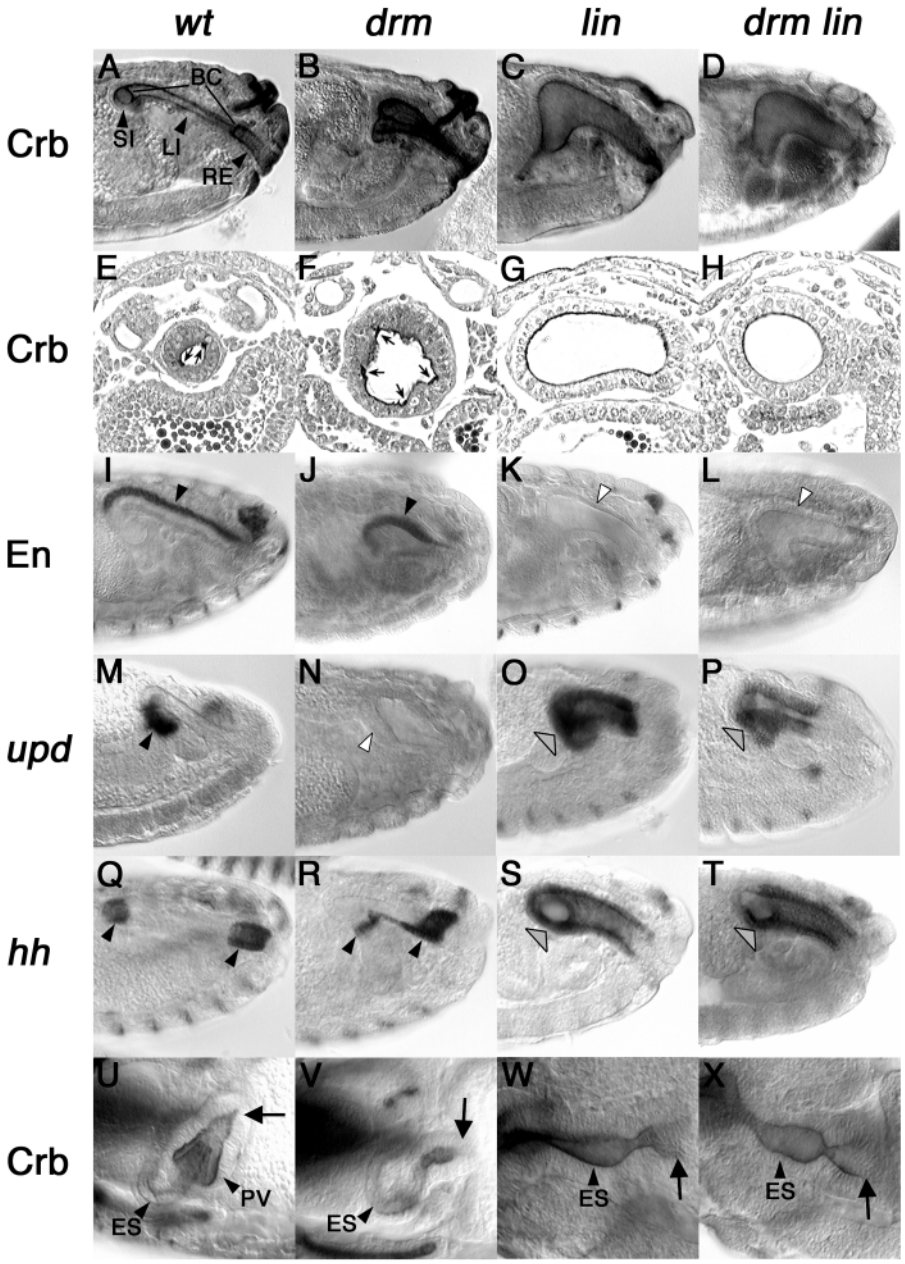

Fig. 1. *lin* is epistatic to *drm*. Whole-mount embryos were stained with anti-Crb (A-H,U-X) or anti-En (I-L), hybridized in situ with probes for *upd* (M-P) or *hh* (Q-T), or fixed and sectioned transversely (E-H). The wild-type hindgut (A) consists of three morphologically distinct domains: small intestine (SI), large intestine (LI), and rectum (RE). Boundary cell (BC) rings, labeled strongly with anti-Crb, separate the SI and LI anteriorly and the LI and RE posteriorly. Two boundary cell rows also run the length of the LI dividing it dorsoventrally, as seen in transverse section (two arrows in E). In *drm* embryos (B), the SI is missing, the cells of the LI are columnar, and the BC rows are duplicated (four arrows in F). In both *lin* (C,G) and *drm lin* (D,H) embryos, the LI is missing, the cells are cuboidal, and the BC rows are absent. In wild-type embryos, En is expressed in the dorsal portion of the LI (I, black arrowhead). In *drm* embryos (J), En is expressed throughout dorsal hindgut (black arrowhead), but is not expressed in the rectum. In *lin* (K) and *drm lin* (L) embryos, En-expressing cells are not present (white arrowhead). In wild-type embryos (M, arrowhead), *upd* is expressed within the SI. In *drm* embryos (N), *upd* is not expressed (white arrowhead). In *lin* (O) and *drm lin* (P) embryos, expression of *upd* is expanded throughout most of the hindgut (wide arrowhead), but not the RE. In wild-type embryos, *hh* is expressed in both the SI and RE (Q, arrowheads). In *drm* embryos (R), *hh* is expressed in the RE, the ventral portion of the LI, and at the junction between the hindgut and midgut (arrowheads). In *lin* (S) and *drm lin* (T) embryos, expression of *hh* is expanded throughout most of the hindgut (wide arrowhead), but not the RE. In Crb-stained wild-type embryos (U), the proventriculus (PV) forms a multi-layered valve-like structure between the esophagus (ES) and anterior midgut (arrows in U-X indicate junction with anterior midgut). In *drm* embryos (V), the PV does not fold properly. In both *lin* (W) and *drm lin* (X) embryos, the entire foregut appears shorter and wider, and the PV does not form (arrows).

Table 1. Mutations in the *drm* gene

Allele	Mutation	Location	Gut defects
drm^{1}	I element insertion*	35 bp upstream of transcription start	PV, HG
drm^{2}	R46H (C<u>G</u>C→C<u>A</u>C)†	1st zinc finger	PV
drm^{3}	*roo* element insertion‡	At exon 2 splice donor site	PV, HG
drm^{4}	E45K (<u>G</u>AG→<u>A</u>AG)†	1st zinc finger	PV
drm^{5}	E25K (<u>G</u>AG→<u>A</u>AG)†	1st zinc finger	PV
drm^{6}	R46C (<u>C</u>GC→<u>T</u>GC)†	1st zinc finger	PV, HG
Df(2L)drm^{P1}	97 kb deletion from *l(2)k10101* through *drm*§	Deletion of *drm*	PV, HG
Df(2L)drm^{P2}	165 kb deletion from *l(2)k10101* through *l(2)k06860*§	Deletion of *drm*, *sob* and *odd*	PV, HG

Generation of *drm* mutations and phenotypic characterization are discussed in text. PV, proventriculus; HG, hindgut.
*See Fig. 2B for insertion location.
†Altered nucleotide is underlined, see Figs 2D and 3C for residue location.
‡See Fig. 3C for insertion location.
§See Fig. 2A for deletion breakpoints.

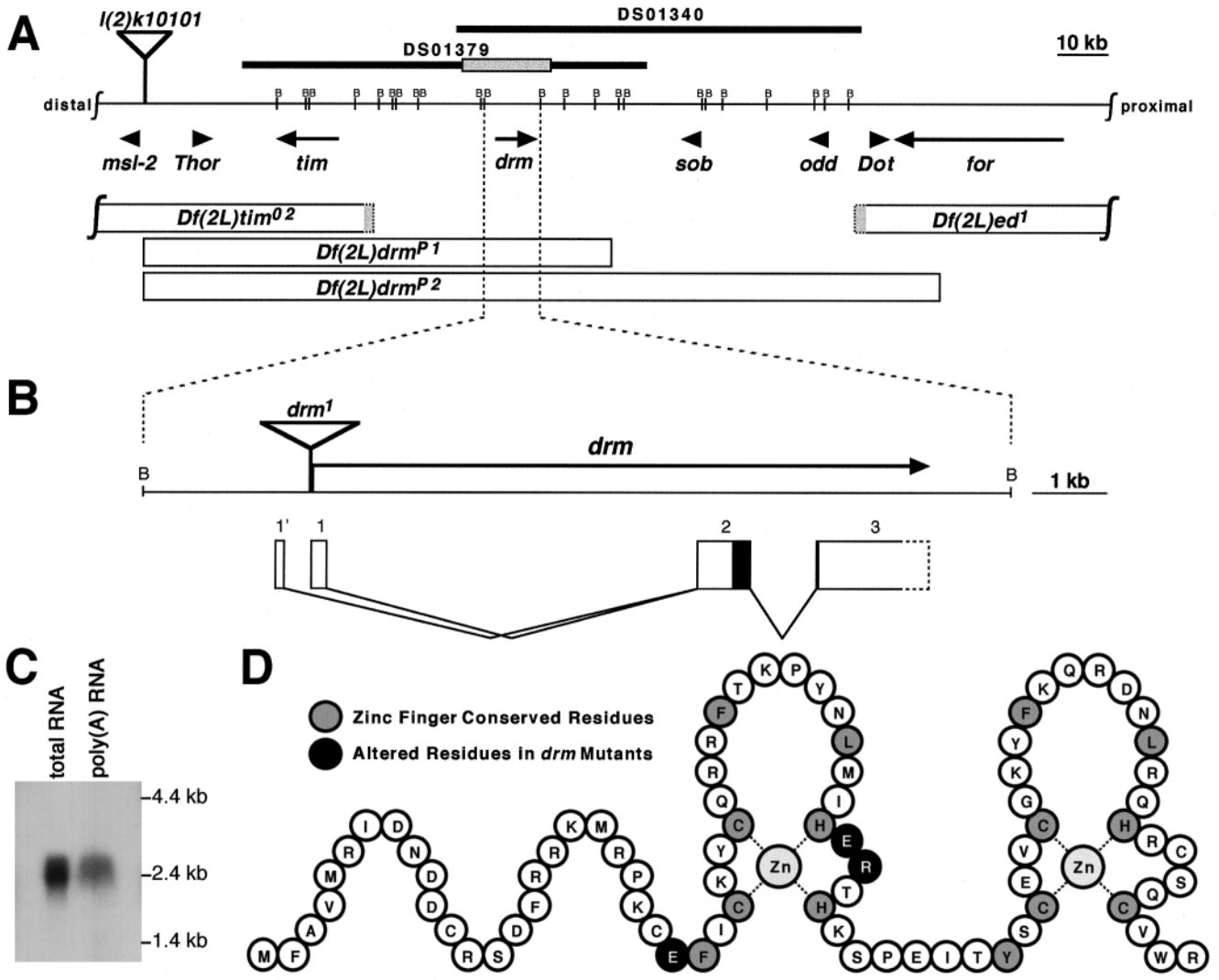

Fig. 2. Molecular characterization of *drm*. (A) Physical map between *male-specific lethal-2* (*msl-2*) and *foraging* (*for*) (cytological regions 23F3 to 24A3). Genomic DNA in P1 phage clones DS01379 and DS01340 is shown above the map, with the 18.1 kb fragment used for genomic rescue experiments shaded in gray. Characterized genes are shown with arrows representing their directions of transcription, as annotated in GadFly (Rubin et al., 2000b). The *l(2)k10101* P element, mobilized to generate deficiency alleles, is represented by an inverted triangle. Below, deficiencies are represented by open bars with breakpoint uncertainties shown in gray. *Df(2L)tim*^{02} and *Df(2L)ed*^{1} were used for rough mapping of the *drm*^{1} allele. The breakpoints of *Df(2L)drm*^{P1} and *Df(2L)drm*^{P2} were mapped molecularly. B, *Bam*HI. (B) Expanded view of the 11.9 kb *Bam*HI fragment that includes the *drm* gene. The I element in the *drm*^{1} chromosome is inserted 35 bp upstream of the transcription start site. The *drm* transcription unit is 8.5 kb with three exons spliced together to form a 2.5 kb mRNA. An alternate first exon (1′) was found in 10% of 5′ RACE products, and several alternate transcriptional stop sites (dotted lines in exon 3) were present in 3′ RACE products. The *drm* ORF (black) spans the second splice junction. (C) Northern blot of 50 μg total embryonic RNA (0-17 hours) and 1 μg poly(A) RNA shows the approximately 2.5 kb *drm* mRNA. (D) Schematic representation of the Drm protein folded to form one C_2H_2 and one C_2HC zinc finger. Residues conserved in the canonical C_2H_2 zinc finger are shaded gray and residues altered in the *drm* point mutants are black (see Table 1).

products, and genomic DNA (Adams et al., 2000) is consistent with the conclusion that CG10016 is an 8.5 kb transcription unit. Three exons are spliced to form a 2.5 kb mRNA encoding an 81 amino acid, 10,120 Da predicted protein (Wilkins et al., 1998).

The position of the I element in *drm*^{1}, and the endpoints of the deletions in *drm*^{P1} and *drm*^{P2}, strongly suggest that CG10016 is the *drm* gene. To obtain further evidence supporting this relationship, we performed rescue and mutagenesis experiments. We generated germline transformants of an 18.1 kb fragment of genomic DNA (Fig. 2A) that includes CG10016 plus 6.9 kb of upstream and 2.7 kb of downstream DNA (but no other predicted genes). Although this construct does not rescue *drm* lethality, it does rescue the *drm* hindgut and foregut phenotypes (data not shown). We also generated and molecularly characterized five new EMS-induced alleles (see Materials and Methods). Four of these are point mutations (in three different residues) within the first zinc finger, and one is a *roo* element insertion in the second exon splice donor site (Fig. 2D, Table 1); no mutations were found outside the ORF. In all of these mutants, the proventriculus is both morphologically and functionally defective (assessed by

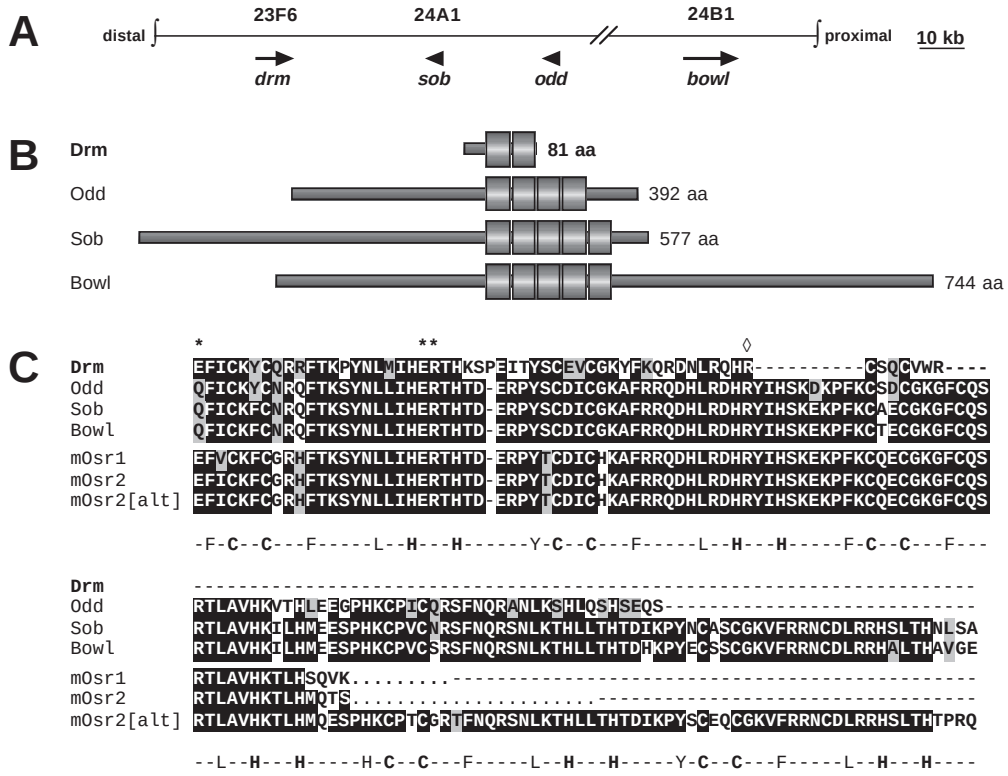

Fig. 3. Drumstick is a member of the Odd-skipped family of zinc finger proteins. Cytological map showing the proximity of *drm*, *sob*, *odd* and *bowl* (A). Drm, Odd, Sob and Bowl are similar in their zinc finger domains, but otherwise share little sequence similarity; protein lengths are indicated to the right (B). Alignment of the zinc fingers from Drm, Odd, Sob, and Bowl (C). The zinc fingers from *Mus musculus* mOsr1 and mOsr2 (and its alternatively spliced form, mOsr2[alt]), are shown for comparison (mouse and human Osr proteins are identical within the zinc finger motifs). Identical and similar residues are shaded black and gray, respectively (BOXSHADE, v. 3.2). Dashes indicate gaps in the alignment, and dots indicate amino acid residues (not shown) outside the zinc finger domains. Conserved residues in the canonical C_2H_2 zinc finger are shown below. Asterisks above the Drm sequence denote single residues altered in *drm* mutants (see Table 1 and Fig. 2D), and the diamond denotes the second exon splice donor site where the *drm*^{3} *roo* element is inserted.

larval feeding assays; data not shown), while the hindgut is defective only in flies carrying the stronger alleles. These phenotypic characteristics support the following allelic series: *drm*^{5}<*drm*^{2}<*drm*^{4}<*drm*^{1}<*drm*^{3}=*drm*^{6}<*drm*^{P1}=*drm*^{P2}. Based on phenotypic rescue experiments and molecular mapping of *drm* alleles, we conclude that CG10016 is the *drm* gene.

Drm is a member of the *Drosophila odd-skipped* (*odd*) family of zinc finger encoding genes that includes *odd*, *sister of odd and bowl* (*sob*), and *bowel* (*bowl*) (Nüsslein-Volhard and Wieschaus, 1980; Coulter et al., 1990; Hart et al., 1996; Wang and Coulter, 1996). These genes map close to each other (Fig. 3A), suggesting that the family has arisen by relatively recent duplication. Like *bowl* and *sob* (but not *odd*), *drm* contains a splice donor site within the R74 codon of the second zinc finger. Interestingly, this splice site has been conserved evolutionarily, as it is also present in both the mouse and human *odd-skipped related* (*Osr*) genes *Osr1* and *Osr2* (So and Danielian, 1999; Lan et al., 2001).

The Drm protein contains two zinc finger motifs (compared to four in Odd and five in both Sob and Bowl; Fig. 3B). The zinc fingers in Odd, Sob, and Bowl conform to the canonical C_2H_2 structure (C-X_2-C-X_{12}-H-X_3-H) that is most commonly associated with a DNA-binding function, but in some cases, can have protein-binding capability (Rosenfeld and Margalit, 1993; Mackay and Crossley, 1998). In Drm, the first zinc finger conforms to the canonical C_2H_2 sequence and has a high degree of similarity (~95%) to the first finger of the other Odd family members. The second zinc finger of Drm is divergent; the primary sequence conforms to the canonical C_2H_2 sequence up to the H73 residue, but the second His residue is replaced by a Cys, with H-X_4-C spacing between the latter two zinc-coordinating residues. This residue spacing is found in other C_2HC fingers with demonstrated protein-binding activity. Computer modeling (SWISS-MODEL) (Guex and Peitsch, 1997) with respect to the known structure of the *Drosophila* U-shaped (Ush) C_2HC zinc finger shows that the Drm C_2HC finger is theoretically capable of folding around a zinc ligand (Liew et al., 2000). Another distinguishing feature of Drm is the divergent linker region between its zinc fingers. The most common linker, found in over 50% of known C_2H_2 fingers, consists of five residues with the consensus sequence TG(E/Q)(K/R)P (Wolfe et al., 2000). The Odd, Sob and Bowl linkers all have the conserved sequence TDERP, whereas the Drm linker (KSPEIT) is different both in sequence and length (Fig. 3C). Since its C_2H_2 and C_2HC zinc fingers are, in principle, capable of either DNA or protein binding, Drm may function by either or both of these mechanisms.

Expression of *drm* during embryogenesis

Consistent with the gut defects observed in *drm* embryos, *drm* is expressed dynamically in cells that will give rise to the foregut and hindgut (Fig. 4). In the posterior gut primordium, *drm* mRNA is first detected at stage 5 in a ventral crescent at 10% embryo length (EL) (Fig. 4A). Cells in this region are fated to give rise to the epithelia of the posterior midgut, Malpighian tubules and hindgut (Campos-Ortega and Hartenstein, 1997). At stage 6, the posterior crescent expands dorsally to encircle the amnioproctodeal plate (Fig. 4B). By stage 7, *drm* is expressed in a ring within the proctodeal invagination (Fig. 4C). During germ band extension (stages 8

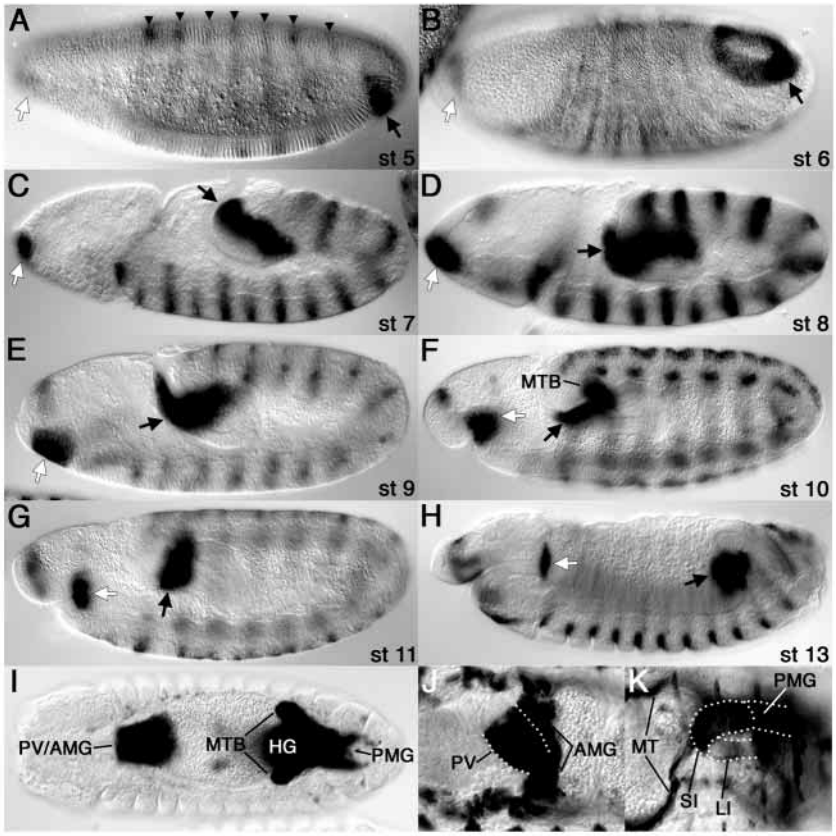

Fig. 4. Expression of *drm* during embryogenesis. Whole-mount in situ hybridization with *drm*-specific probe shows the dynamic expression pattern of *drm* between embryonic stages 5 and 13 (A-H). *drm* expression is first observed at stage 5 in a ventral crescent in the posterior midgut-hindgut primordium (at 10% EL), a weakly stained anterior spot in the foregut-proventriculus primordium (at 95-100% EL) (black and white arrows in A-H indicate expression in posterior and anterior gut, respectively), and in seven transverse stripes (arrowheads; A). By stage 6, the posterior crescent has expanded to encircle the amnioproctodeal plate (B, dorsolateral view), and secondary transverse stripes arise between the initial seven to give a total of 14. Between stages 7 and 9, *drm*-expressing cells internalized with the proctodeal invagination are located at the midgut-hindgut junction (C-E). At stage 10, *drm* is expressed in the invaginating stomodeum and transiently in the Malpighian tubule buds (F). Between stages 11 and 13, *drm* expression is refined to the posterior midgut, the ureters of the Malpighian tubules, the anterior small intestine, the proventriculus anlage, and at the anterior boundary of each segment. Expression is also observed in the pharynx and stigmatophore. Whole-mount *drm*-GAL4:UAS-*lacZ* embryos stained with anti-β-gal (I-K) reveal, by stage 13, *lacZ* expression in more extensive domains (both anteriorly and posteriorly) than those seen for *drm* mRNA expression at the same stage (I, dorsal view; compare Fig. 4H). At stage 16 (J and K, higher magnification), β-gal is present throughout the entire proventriculus, anterior midgut, posterior midgut, Malpighian tubules, and small intestine. Dotted lines outline the proventriculus (J), posterior midgut, small intestine, and large intestine (K). MTB, Malpighian tubule buds; MT, Malpighian tubules; PV, proventriculus; AMG, anterior midgut; PMG, posterior midgut; HG, hindgut; SI, small intestine; LI, large intestine.

and 9), *drm* expression is seen in a region overlapping the junction of the posterior midgut and hindgut primordia (Fig. 4D,E). At stage 10, *drm* is expressed transiently in the evaginating buds of the Malpighian tubules (Fig. 4F). Between stages 11 and 13, *drm* mRNA is detected in the posterior midgut, the ureters of the Malpighian tubules, and the most anterior cells of the small intestine (Fig. 4G,H); expression in these domains persists throughout the remainder of embryogenesis.

drm is also expressed in the anterior gut primordium starting at stage 5 (Fig. 4A). Expression increases in this domain until stage 10 when it is internalized as the invaginating stomodeum (Fig. 4F). *drm* expression is then refined to a narrow ring of cells at the junction of the foregut and anterior midgut (Fig. 4H). Like *odd* and *sob* (Hart et al., 1996), *drm* is also expressed in a seven-stripe segmental pattern at stage 5 (Fig. 4A); this pattern evolves into fourteen stripes that mark the anterior margin of each segment (Fig. 4H).

The domains in which *drm* is expressed during embryogenesis include a region predicted to become small intestine (Fig. 4C-G). By stage 13, however, *drm* mRNA is not seen in the small intestine (Fig. 4H). To determine if *drm* is expressed early in cells fated to become small intestine, we generated a *drm*-GAL4 driver and used it to drive UAS-*lacZ*. Owing to the perdurance of both GAL4 and β-gal, this provides an historical summation of the *drm* expression pattern. By stage 13, β-gal is detected in a much larger domain of the posterior gut in *drm*-GAL4:UAS-*lacZ* embryos than is *drm* mRNA in wild-type embryos (Fig. 4I, compare with 4H). Most importantly, the presence of β-gal in the small intestine of stage 16 embryos (Fig. 4K) demonstrates that some of the *drm*-expressing cells in the early embryo do indeed give rise to the small intestine.

drm and *lin* interact in vivo

If, as suggested above, spatially localized expression of *drm* in the anterior hindgut allows specification of the small intestine by antagonizing *lin*, then expression of *drm* throughout the hindgut should inhibit endogenous *lin*, thereby producing a *lin*-like hindgut phenotype. We tested this by driving UAS-*drm* using the hindgut-specific *byn*-GAL4 driver. The result of this gain-of-function expression of *drm* is a hindgut phenotype that resembles *lin* loss-of-function mutants: the hindgut is short and distended, consisting of a uniform layer of cuboidal cells similar to those of the wild-type small intestine, and the boundary cell rows are absent (Fig. 5A,C). *en* is not expressed in the hindgut of these embryos, but *upd* and *hh* expression is greatly expanded posteriorly (Fig. 5E,G,I). Like *lin* mutations, the *byn*-GAL4:UAS-*drm* combination is lethal. Overall, it appears that in both *lin* mutants and embryos expressing *drm* throughout the hindgut the small intestine is expanded at the expense of the large intestine. We conclude that *drm* functions in the hindgut by antagonizing *lin*.

If *drm* acts primarily by inhibiting *lin* activity in the hindgut,

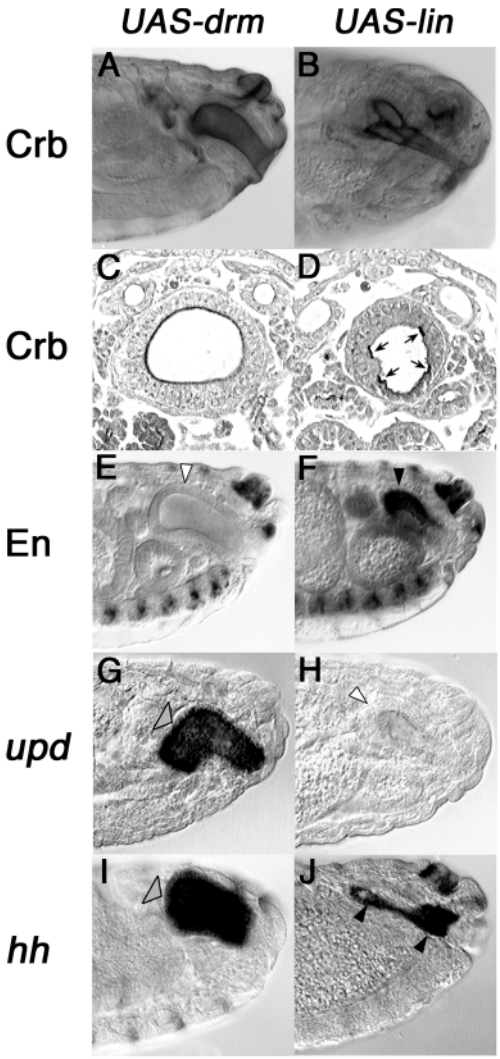

Fig. 5. Drm and Lin antagonize each other in vivo. Whole-mount embryos were stained with anti-Crb (A-D) or anti-En (E,F), hybridized in situ with probe for *upd* (G,H) or *hh* (I,J), or fixed and sectioned transversely (G,H). Ectopic expression of Drm throughout the hindgut with the *byn*-GAL4 driver produces a *lin*-like phenotype as observed by morphology of the hindgut (A; compare Fig. 1C), by hindgut epithelial cell shape and absence of boundary cell rows (C; compare Fig. 1G), by the lack of expression of En in the large intestine (E, white arrowhead; compare Fig. 1K), and by the posterior expansion of *upd* and *hh* from the small intestine (G and I, wide arrowheads; compare Fig. 1O and 1S). Ectopic expression of Lin throughout the hindgut using the *byn*-GAL4 driver produces a *drm*-like phenotype as observed by the morphology of the hindgut (B; compare Fig. 1B), hindgut epithelial cell shape and duplication of boundary cell rows (D, four arrows, compare with Fig. 1F), the expression of En in the dorsal large intestine (F, black arrowhead; compare Fig. 1J), the absence of *upd* expression in the small intestine (H, white arrowhead; compare Fig. 1N), and the expression pattern of *hh* (J, black arrowheads; compare Fig. 1R).

then overexpression of *lin* might overcome the repressive effect of endogenous *drm*, thereby producing a *drm*-like phenotype. Consistent with this notion, overexpression of *lin* produces a hindgut phenotype that resembles *drm* loss-of-function mutants: the hindgut is short and wide, consisting of an undulating layer of columnar cells with a duplication of the boundary cell rows (Fig. 5B,D). As seen in *drm* embryos, *en* is expressed throughout the dorsal hindgut, *upd* expression is absent, and *hh* expression in the small intestine is reduced (Fig. 5F,H,J). Like *drm* mutations, the *byn*-GAL4:UAS-*lin* combination is lethal. Since weaker hindgut drivers (e.g. *14-3fkh*-GAL4) and weaker UAS-*lin* transformants do not produce a phenotype as severe as with the strong *byn*-GAL4 driver or the strongest UAS-*lin* stocks (R. Green, unpublished observations), we conclude that the repressive effect of *drm* can be titrated only by relatively high levels of *lin*.

Drm interacts physically with Lin

The epistasis and in vivo overexpression studies indicate that *drm* inhibits *lin* activity, either directly or indirectly. As we observe no reduction of *lin* expression in the *drm* expression domains of wild-type embryos (Hatini et al., 2000; Iwaki et al., 2001), or any changes in *drm* or *lin* expression in *lin* or *drm* mutant embryos, respectively (data not shown), we conclude that *drm* does not affect *lin* at the transcriptional level. We therefore used a biochemical approach to ask whether Drm might interact physically with Lin. When expressed together in cultured cells, full-length Drm and full-length Lin interact with each other, as demonstrated by coimmunoprecipitation assays (Fig. 6B, lane 1), indicating that the two proteins are in a complex. Since Drm and Lin interact with each other in a yeast two-hybrid assay (data not shown), the Drm-Lin interaction is likely mediated by direct binding.

To map the protein interaction domain, we generated deletion and point mutation constructs of Drm (Fig. 6A) and tested their ability to coimmunoprecipitate with Lin (Fig. 6B). The N-terminal portion of Drm (N-Drm) is unable to bind Lin, while the C-terminal portion of Drm, containing the two zinc finger motifs (C-Drm), retains full Lin-binding activity. Because these results map the protein-protein interaction domain to the zinc fingers, we tested the requirement of each individual zinc finger for Lin-binding activity. A mutation in the C_2H_2 first finger (R46C, identical to the mutation in the drm^6 null allele) abolishes Lin-binding activity, while disruption of the C_2HC second finger (C57G, a substitution in one of the conserved zinc-binding cysteine residues) reduces Lin-binding activity, but does not abolish it completely. To confirm these results, we made similar point mutations in the truncated C-Drm construct and tested their effect on Lin-binding activity. Again, a mutation in the C_2H_2 first finger in C-Drm(R46C) abolishes Lin-binding activity while disruption of the C_2HC second finger in C-Drm(C57G) reduces Lin-binding activity (Fig. 6B). We conclude that the C_2H_2 zinc finger is essential for binding to Lin, while the C_2HC finger contributes to binding, perhaps by stabilizing the interaction.

Structure-function analysis of Drm-Lin antagonism in vivo

We next asked which portions of the Drm protein are required to block Lin function in vivo by expressing, throughout the hindgut, the same Drm deletion and point mutation constructs used in the coimmunoprecipitation studies (Fig. 6A). We assayed the activity of these mutated proteins by their ability to induce a *lin*-like hindgut

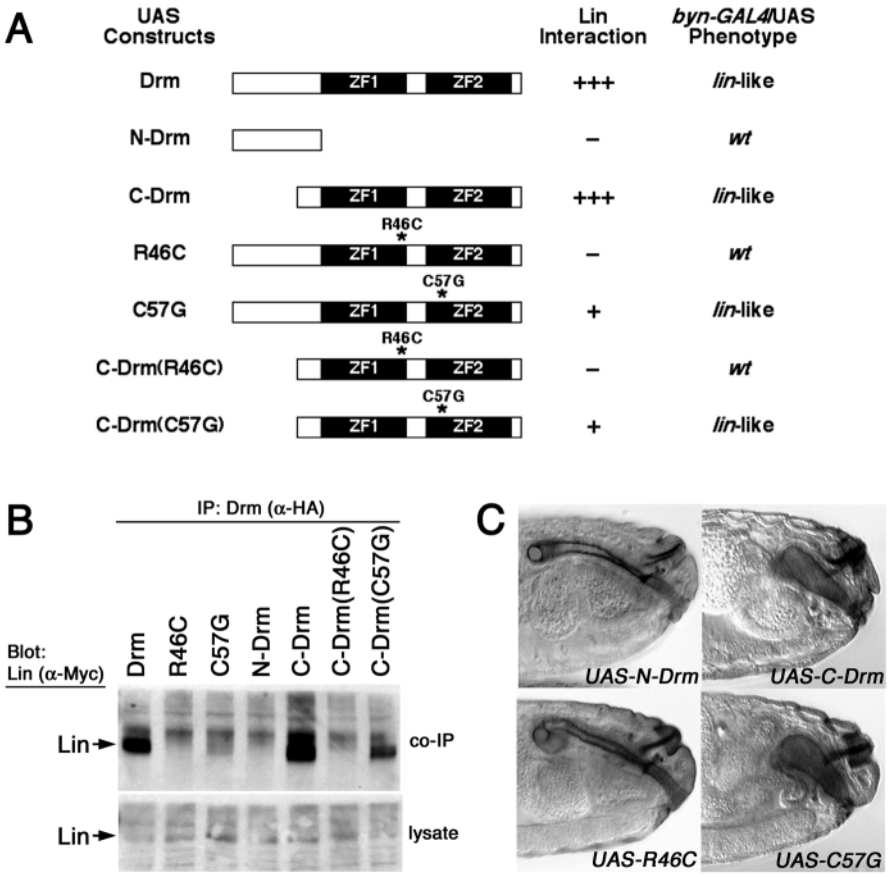

Fig. 6. Structure-function analysis of Drm-Lin interaction in vitro and in vivo. (A) Drm constructs. The full-length, wild-type Drm construct contains two zinc fingers (ZF1 and ZF2). The N-Drm construct consists of the 25-residue N-terminal portion of Drm, and the C-Drm construct contains the C-terminal 63-residue domain, including the two zinc fingers. R46C is the strong *drm*^{6} missense mutation within ZF1, and C57G is a missense mutation in one of the conserved zinc-binding Cys residues of ZF2. The ability of each derivative to bind Lin in vitro was determined by coimmunoprecipitation of epitope-tagged Drm and Lin from Schneider S2 cells (B). Lin binds with high affinity to full-length Drm and C-Drm, with lower affinity to C57G and C-Drm(C57G), and does not bind to N-Drm, R46C, or C-Drm(R46C). Control samples of cell lysates show that Lin was expressed in all transfection assays. To assess the effect of these constructs in vivo, *byn*-GAL4 was used to drive expression of each throughout the hindgut, and the phenotype characterized by anti-Crb staining (C). Expression of N-Drm results in a wild-type appearing hindgut, while expression of C-Drm produces a *lin*-like phenotype similar to the gain-of-function phenotype produced by ectopic expression of full-length Drm (compare Fig. 5A). Expression of R46C results in a wild-type hindgut while C57G produces a *lin*-like phenotype. +++ or +, strong or weak interaction, respectively; –, no interaction.

phenotype when ectopically expressed with *byn*-GAL4 (similar to the gain-of-function phenotype induced by ectopic expression of full-length Drm). Expression of N-Drm, which lacks the zinc fingers, results in a morphologically wild-type hindgut (Fig. 6C), while expression of C-Drm, which contains only the zinc finger motifs, produces a morphologically *lin*-like hindgut (i.e. short and distended and lacking boundary cell rows; Fig. 6C, compare with Fig. 5A). Because these results map the in vivo Lin-inhibiting activity to the zinc fingers, we tested the requirement of each individual zinc finger for Lin-inhibiting activity. A mutation in the C_2H_2 first finger (R46C) abolishes the Drm gain-of-function phenotype, while disruption of the second C_2HC finger (C57G) has no effect on Drm activity (Fig. 6C, compare with Fig. 5A). These effects are observed whether the point mutations are in full-length Drm (R46C and C57G) or in the truncated C-terminal portion of Drm (C-Drm(R46C) and C-Drm(C57G); data not shown). Taken together, the results demonstrate that the first zinc finger, but not the second, is required for Lin-inhibiting activity in vivo.

In summary, Drm constructs that coimmunoprecipitate with Lin are able to repress *lin* activity in vivo, while Drm constructs lacking Lin-binding activity in vitro are not able to repress *lin* activity in vivo (see Fig. 6A). We conclude that the C_2H_2 first finger is essential for both the Lin-binding and Lin-antagonizing functions of Drm. The C_2HC second finger, while contributing to Lin binding, is not absolutely required for Lin-inhibiting activity. Thus the *drm* and *lin* antagonism observed by genetic approaches is mediated by a physical interaction between the Drm and Lin proteins.

DISCUSSION

Drm relief of Lin repression is required for both patterning and cell rearrangement in the hindgut

We showed previously that *drm* is required for specification of the small intestine, while *lin* represses this fate (Iwaki et al., 2001). Here we demonstrate that *lin* is epistatic to *drm*, indicating that *lin* acts downstream of *drm* in a genetic pathway. In our molecular characterization, we determine that, in contrast to the uniform expression of *lin* (Hatini et al., 2000), *drm* is expressed in a highly localized pattern at the anterior of the hindgut primordium. We further show that uniform expression of *drm* throughout the hindgut results in a *lin*-like phenotype. When co-expressed in cultured cells, Drm and Lin are found in a complex. Taking into account these genetic, molecular and biochemical data, we propose a model (Fig. 7) in which Lin (or a complex containing Lin) functions as a transcriptional regulator that represses the genetic program promoting small intestine fate. In the anterior of the hindgut, Drm blocks the activity of Lin by direct physical association, thereby allowing specification of small intestine fate. The Drm-Lin interaction in the hindgut thus defines a pathway in which the spatially localized expression of a small regulatory protein inhibits the repressive effect of a uniformly expressed transcriptional regulator.

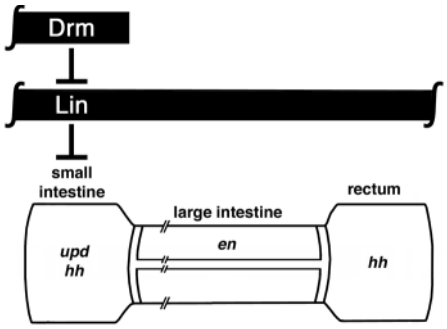

Fig. 7. Model for small intestine specification by Drm-mediated relief of Lin repression. Lin is expressed broadly throughout the hindgut primordium and represses small intestine fate. Drm expression is localized to the anterior hindgut primordium where it represses Lin activity, thereby allowing the small intestine to be specified. See text for details.

Putative transcriptional regulators have been shown to be required for a number of processes of epithelial cell rearrangement. *die-1* encodes a zinc finger protein required for intercalation of dorsal epidermal cells in *C. elegans* (Heid et al., 2001), *grain* a GATAc factor required for stigmatophore elongation (Brown and Castelli-Gair Hombría, 2000), and *ribbon* (*rib*) a BTB domain protein required for tracheal branching morphogenesis (Bradley and Andrew, 2001). All of these genes are expressed throughout and are required within the cells undergoing cell rearrangement. In contrast, *drm* is expressed only at one end of the prospective hindgut, but is required for cell rearrangement throughout much of the epithelium.

As the *drm*, *bowl* and *lin* phenotypes suggest that juxtaposition of properly specified small and large intestine is required for hindgut cell rearrangement (Iwaki et al., 2001), we speculate that expression of signaling molecules specifically in the small intestine orients the rearrangement of cells within the large intestine. Hedgehog (Hh), Wingless (Wg) and Serrate (Ser) are expressed in the termini of the hindgut, but they appear to play either a minor or no role in controlling morphogenesis (Iwaki et al., 2001; Iwaki and Lengyel, 2002). One signaling molecule that is required for hindgut cell rearrangement is Upd, the *Drosophila* ligand activating JAK/STAT signaling, which is expressed specifically in the small intestine (K. A. J. and J. A. L., unpublished). Further characterization of the *upd* pathway and its downstream effectors may provide insight into how patterning of the small intestine affects oriented cell rearrangement.

Drm is a protein-binding member of the Odd-skipped zinc finger family

Both epistasis and ectopic expression experiments indicate that, in the hindgut, Drm acts primarily through Lin. The association between Drm and Lin, demonstrated both in cultured cells and in yeast, suggests that, rather than binding to DNA, Drm functions by binding to protein. Drm contains two zinc fingers that differ structurally, and perhaps functionally, from those of its family members. The first, canonical C_2H_2 finger lacks the conserved TG(E/Q)(K/R)P linker present in other Odd family zinc fingers, which is required in other canonical C_2H_2 fingers for stabilization of high-affinity DNA-protein binding (Laity et al., 2000). Furthermore, as shown here, this C_2H_2 finger is both necessary and sufficient for Lin-binding in vitro and Lin-inhibiting activity in vivo. A protein-binding function for the Drm C_2H_2 finger is consistent with the demonstrated role of other C_2H_2 fingers, including those of the Ikaros family, in homo- and heterodimerization (Sun et al., 1996; Morgan et al., 1997; Kelley et al., 1998). Although we cannot rule out a DNA-binding function for Drm, our data are consistent with a model in which the primary role of the C_2H_2 first finger is in binding to Lin.

C_2HC fingers have also been shown to act as protein binding motifs: both mammalian FOG and *Drosophila* Ush bind to zinc fingers in their partner proteins via specific C_2HC fingers (Tsang et al., 1997; Fox et al., 1999; Haenlin et al., 1997). When co-expressed in cultured cells and assessed by coimmunoprecipitation, the Drm C_2HC second finger does indeed contribute to the binding of Drm to Lin (although it is not absolutely necessary). In overexpression studies in vivo, however, the Drm C_2HC finger was not necessary for Lin-inhibiting activity. Consistent with this in vivo observation, no mutations in the Drm C_2HC finger were identified in our screen of 18,000 mutagenized chromosomes. Thus, while a protein-binding function is suggested by the in vitro data, we have not detected a required in vivo function for the Drm C_2HC finger.

In conclusion, our characterization of Drm adds to the growing number of C_2H_2 zinc fingers that act as protein-protein interaction motifs (Mackay and Crossley, 1998). The Drm protein is unique in that it is extremely small (10 kDa), is expressed in a highly spatially localized pattern, and appears to function entirely (at least in the hindgut) by associating with, and thereby antagonizing, the activity of a globally expressed protein, Lin.

Globally-expressed Lin requires spatially localized cofactors for specificity

lin is expressed relatively uniformly throughout the embryo, yet has tissue- and stage-specific effects, and both activating and repressing activities. A number of these functions have been shown to depend on spatially localized cofactors or signals. In the posterior spiracles and eighth abdominal belt, *lin* functions together with *Abdominal B* (which is expressed specifically in the posterior) to activate *empty spiracles*, *cut* and *spalt* (Castelli-Gair, 1998). In the dorsal epidermis, as a result of localized *wg* signaling, *lin* activates *wg* and represses *veinlet* expression (Hatini et al., 2000); *lin* is required to promote quaternary (4°) and represses tertiary (3°) cell fates (Bokor and DiNardo, 1996; Hatini et al., 2000). In the hindgut, *lin* represses expression of *upd* and *hh* (characteristic of small intestine fate); establishment of the small intestine requires the locally expressed cofactor Drm, which relieves repression by Lin.

Antagonism of repressors is an important mechanism by which transcriptional activity is spatially regulated (Courey and Jia, 2001). In *Drosophila*, localized cell signaling by receptor tyrosine kinases (e.g. Torso and Sevenless) or the canonical *wg* pathway is required to relieve global repression (in a number of cases by Groucho), thereby allowing proper patterning and/or differentiation of portions of the embryonic termini, segments, midgut and eye (Paroush et al., 1997; Jimenez et al., 2000; Waltzer and Bienz, 1998; Cavallo et al., 1998; Rebay and Rubin, 1995). While these relief-of-repression pathways are

dependent on localized cell signaling, the Drm-Lin interaction is, to our knowledge, the first described example in which relief of repression is initiated by spatially restricted production of a small transcriptional regulator.

Many questions remain about the Drm-Lin interaction and its mechanism of action. First, it is not clear how Lin acts as a transcriptional regulator. In the hindgut, and perhaps in other tissues, Lin might act as part of a repressosome complex (Courey and Jia, 2001), binding DNA directly or associating with chromatin on the basis of an interaction with other DNA-binding proteins. Binding of Drm to a Lin-containing complex might then inhibit the repressive activity of Lin. Second, activation of gene expression requires not only the absence (or inactivation) of repressors, but also the presence of transcriptional activators (Struhl, 1999). Thus, there must be as-yet-unidentified transcriptional activators that promote expression of small intestine-specific targets once Drm has lifted the repression by Lin.

Drm and Lin in other developmental contexts

We have shown that *drm* is expressed dynamically not only in the hindgut, but also in the foregut and in the developing epidermis. This raises the question of whether Drm-mediated Lin inhibition might occur in tissues other than the hindgut. Both the spatially restricted expression of *drm* and the epistasis of *lin* to *drm* in the foregut epithelium (Fig. 1U-X) are consistent with the idea that Drm also blocks Lin activity in the proventriculus primordium, thus allowing proper folding morphogenesis. In the dorsal epidermis, stripes of *drm* expression roughly correspond to defects in patterning seen in *drm* mutants (V. H. and S. DiNardo, unpublished observations); these defects are opposite to those seen in *lin* embryos (Hatini et al., 2000), suggesting that Drm-mediated relief of Lin repression may occur in dorsal epidermis patterning. We have also observed *lin* expression in leg imaginal discs and a required role for *lin* in leg development (V. Hatini and S. DiNardo, unpublished observations); taken together with the potential role of *drm* in the developing leg (Cohen et al., 1991), these results suggest that Drm and Lin might also control aspects of leg development. We conclude that, by antagonizing Lin, Drm controls multiple events of epithelial patterning and thereby morphogenesis.

Another gene in the *odd* family, *bowl*, has a hindgut phenotype very similar to that of *drm* (Wang and Coulter, 1996; Iwaki et al., 2001), suggesting that *bowl* might also function in the same pathway as *drm* and *lin*. However, in contrast to the spatially localized expression of *drm*, but similar to the spatial and temporal expression of *lin*, *bowl* expression appears uniform throughout the hindgut primordium until stage 12 (Wang and Coulter, 1996). Thus, despite its similarity in both mutant phenotype and sequence to *drm*, *bowl* function in the hindgut is likely different from that of *drm*. In mouse and humans, the genes *Osr1* and *Osr2* encode Odd-related proteins with three and five zinc fingers, respectively, that are most similar to those of Sob and Bowl (Fig. 3C) (So and Danielian, 1999; Lan et al., 2001). Mouse *Osr1* and *Osr2* are expressed during embryogenesis in dynamic, spatially localized patterns correlated with sites of active morphogenesis (So and Danielian, 1999; Lan et al., 2001). Given that Drm (and perhaps Bowl) is involved in a pathway with Lin, it may be significant that a mammalian protein, predicted from an EST clone and sharing homology with Lin over a 200 amino acid region, was recently identified (Venter et al., 2001). It will be interesting to determine if any parallels exist between the expression and function of these mammalian homologs and the *Drosophila* Lin and Odd family of proteins.

We thank Silvia Wenjuan Yu and Monica Martinez for excellent technical assistance, Joan Hooper for assistance in making the UAS-DrmEST germline transformant, the Bloomington Stock Center for fly stocks, Albert J. Courey, Utpal Banerjee, Cheryl Kerfeld and members of the Lengyel laboratory for helpful discussions, and Stephen DiNardo for his encouragement, active participation and support to V. H. This work was supported by NIH grants GM08042 to the UCLA Medical Scientist Training Program (to support R. B. G.), GM45747 to S. DiNardo (to support V. H.), and HD09948 to J. A. L.

REFERENCES

Adams, M. D., Celniker, S. E., Holt, R. A., Evans, C. A., Gocayne, J. D., Amanatides, P. G., Scherer, S. E., Li, P. W., Hoskins, R. A., Galle, R. F. et al. (2000). The genome sequence of *Drosophila melanogaster*. *Science* **287**, 2185-2195.

Ashburner, M. (1989). *Drosophila: A Laboratory Manual*. Cold Spring Harbor, NY: Cold Spring Harbor Laboratory Press.

Bokor, P. and DiNardo, S. (1996). The roles of *hedgehog*, *wingless* and *lines* in patterning the dorsal epidermis in *Drosophila*. *Development* **122**, 1083-1092.

Bradley, P. L. and Andrew, D. J. (2001). *ribbon* encodes a novel BTB/POZ protein required for directed cell migration in *Drosophila melanogaster*. *Development* **128**, 3001-3015.

Brand, A. H. and Perrimon, N. (1993). Targeted gene expression as a means of altering cell fates and generating dominant phenotypes. *Development* **118**, 401-415.

Brown, S. and Castelli-Gair Hombría, J. (2000). *Drosophila grain* encodes a GATA transcription factor required for cell rearrangement during morphogenesis. *Development* **127**, 4867-4876.

Campos-Ortega, J. A. and Hartenstein, V. (1997). *The Embryonic Development of Drosophila melanogaster*. Berlin: Springer-Verlag.

Casso, D., Ramirez-Weber, F. and Kornberg, T. B. (2000). GFP-tagged balancer chromosomes for *Drosophila melanogaster*. *Mech. Dev.* **91**, 451-454.

Castelli-Gair, J. (1998). The *lines* gene of *Drosophila* is required for specific functions of the Abdominal-B HOX protein. *Development* **125**, 1269-1274.

Cavallo, R. A., Cox, R. T., Moline, M. M., Roose, J., Polevoy, G. A., Clevers, H., Peifer, M. and Bejsovec, A. (1998). *Drosophila* Tcf and Groucho interact to repress Wingless signalling activity. *Nature* **395**, 604-608.

Cohen, B., Wimmer, E. A. and Cohen, S. M. (1991). Early development of leg and wing primordia in the *Drosophila* embryo. *Mech. Dev.* **33**, 229-240.

Coulter, D. E., Swaykus, E. A., Beran-Koehn, M. A., Goldberg, D., Wieschaus, E. and Schedl, P. (1990). Molecular analysis of *odd-skipped*, a zinc finger encoding segmentation gene with a novel pair-rule expression pattern. *EMBO J.* **9**, 3795-3804.

Courey, A. J. and Jia, S. (2001). Transcriptional repression: the long and the short of it. *Genes Dev.* **15**, 2786-2796.

Ettensohn, C. A. (1985). Gastrulation in the sea urchin embryo is accompanied by the rearrangement of invaginating epithelial cells. *Dev. Biol.* **112**, 383-390.

Fox, A. H., Liew, C., Holmes, M., Kowalski, K., Mackay, J. and Crossley, M. (1999). Transcriptional cofactors of the FOG family interact with GATA proteins by means of multiple zinc fingers. *EMBO J.* **18**, 2812-2822.

Fuss, B. and Hoch, M. (1998). *Drosophila* endoderm development requires a novel homeobox gene which is a target of Wingless and Dpp signalling. *Mech. Dev.* **79**, 83-97.

Godt, D. and Laski, F. A. (1995). Mechanisms of cell rearrangement and cell recruitment in *Drosophila* ovary morphogenesis and the requirement of *bric á brac*. *Development* **121**, 173-187.

Grigliatti, T. (1986). Mutagenesis. In *Drosophila: A Practical Approach* (ed. D. B. Roberts), pp. 39-58. Oxford: IRL Press.

Guex, N. and Peitsch, M. C. (1997). SWISS-MODEL and the Swiss-PdbViewer: an environment for comparative protein modeling. *Electrophoresis* **18**, 2714-2723.

Haenlin, M., Cubadda, Y., Blondeau, F., Heitzler, P., Lutz, Y., Simpson, P. and Ramain, P. (1997). Transcriptional activity of *pannier* is regulated negatively by heterodimerization of the GATA DNA-binding domain with a cofactor encoded by the *u-shaped* gene of *Drosophila*. *Genes Dev.* **11**, 3096-3108.

Harrison, D. A., McCoon, P. E., Binari, R., Gilman, M. and Perrimon, N. (1998). *Drosophila unpaired* encodes a secreted protein that activates the JAK signaling pathway. *Genes Dev.* **12**, 3252-3263.

Hart, M. C., Wang, L. and Coulter, D. E. (1996). Comparison of the structure and expression of *odd-skipped* and two related genes that encode a new family of zinc finger proteins in *Drosophila*. *Genetics* **144**, 171-182.

Hatini, V., Bokor, P., Goto-Mandeville, R. and DiNardo, S. (2000). Tissue- and stage-specific modulation of Wingless signaling by the segment polarity gene *lines*. *Genes Dev.* **14**, 1364-1376.

Heid, P. J., Raich, W. B., Smith, R., Mohler, W. A., Simokat, K., Gendreau, S. B., Rothman, J. H. and Hardin, J. (2001). The zinc finger protein DIE-1 is required for late events during epithelial cell rearrangement in *C. elegans*. *Dev. Biol.* **236**, 165-180.

Irvine, K. D. and Wieschaus, E. (1994). Cell intercalation during *Drosophila* germband extension and its regulation by pair-rule segmentation genes. *Development* **120**, 827-841.

Iwaki, D. D., Johansen, K. A., Singer, J. B. and Lengyel, J. A. (2001). *drumstick*, *bowl*, and *lines* are required for patterning and cell rearrangement in the *Drosophila* embryonic hindgut. *Dev. Biol.* **240**, 611-626.

Iwaki, D. D. and Lengyel, J. A. (2002). A Delta-Notch signaling border regulated by Engrailed/Invected repression specifies boundary cells in the *Drosophila* hindgut. *Mech. Dev.* **114**, 71-84.

Jimenez, G., Guichet, A., Ephrussi, A. and Casanova, J. (2000). Relief of gene repression by *torso* RTK signaling: role of *capicua* in *Drosophila* terminal and dorsoventral patterning. *Genes Dev.* **14**, 224-231.

Keller, R. E., Danilchik, M., Gimlich, R. and Shih, J. (1985). The function and mechanism of convergent extension during gastrulation of *Xenopus laevis*. *J. Embryol. Exp. Morphol.* **89 Supplement**, 185-209.

Kelley, C. M., Ikeda, T., Koipally, J., Avitahl, N., Wu, L., Georgopoulos, K. and Morgan, B. A. (1998). Helios, a novel dimerization partner of Ikaros expressed in the earliest hematopoietic progenitors. *Curr. Biol.* **8**, 508-515.

Kimmerly, W., Stultz, K., Lewis, S., Lewis, K., Lustre, V., Romero, R., Benke, J., Sun, D., Shirley, G., Martin, C. et al. (1996). A P1-based physical map of the *Drosophila* euchromatic genome. *Genome Res.* **6**, 414-430.

Laity, J. H., Dyson, H. J. and Wright, P. E. (2000). DNA-induced alpha-helix capping in conserved linker sequences is a determinant of binding affinity in Cys_2-His_2 zinc fingers. *J. Mol. Biol.* **295**, 719-727.

Lan, Y., Kingsley, P. D., Cho, E. S. and Jiang, R. (2001). *Osr2*, a new mouse gene related to *Drosophila odd-skipped*, exhibits dynamic expression patterns during craniofacial, limb, and kidney development. *Mech. Dev.* **107**, 175-179.

Laski, F. A., Rio, D. C. and Rubin, G. M. (1986). Tissue specificity of Drosophila P element transposition is regulated at the level of mRNA splicing. *Cell* **44**, 7-19.

Lee, J. J., von Kessler, D. P., Parks, S. and Beachy, P. A. (1992). Secretion and localized transcription suggest a role in positional signaling for products of the segmentation gene *hedgehog*. *Cell* **71**, 33-50.

Lengyel, J. A. and Iwaki, D. D. (2002). It takes guts: the *Drosophila* hindgut as a model system for organogenesis. *Dev. Biol.* **243**, 1-19.

Lengyel, J. A. and Liu, X. J. (1998). Posterior gut development in *Drosophila*: a model system for identifying genes controlling epithelial morphogenesis. *Cell Res.* **8**, 273-284.

Leung, B., Hermann, G. J. and Priess, J. R. (1999). Organogenesis of the *Caenorhabditis elegans* intestine. *Dev. Biol.* **216**, 114-134.

Liew, C. K., Kowalski, K., Fox, A. H., Newton, A., Sharpe, B. K., Crossley, M. and Mackay, J. P. (2000). Solution structures of two CCHC zinc fingers from the FOG family protein U-shaped that mediate protein-protein interactions. *Structure Fold Des.* **8**, 1157-1166.

Liu, X., Kiss, I. and Lengyel, J. A. (1999). Identification of genes controlling malpighian tubule and other epithelial morphogenesis in *Drosophila melanogaster*. *Genetics* **151**, 685-695.

Mackay, J. P. and Crossley, M. (1998). Zinc fingers are sticking together. *Trends Biochem. Sci.* **23**, 1-4.

Montell, D. J. (1999). Developmental regulation of cell migration. Insight from a genetic approach in *Drosophila*. *Cell. Biochem. Biophys.* **31**, 219-229.

Morgan, B., Sun, L., Avitahl, N., Andrikopoulos, K., Ikeda, T., Gonzales, E., Wu, P., Neben, S. and Georgopoulos, K. (1997). Aiolos, a lymphoid restricted transcription factor that interacts with Ikaros to regulate lymphocyte differentiation. *EMBO J.* **16**, 2004-2013.

Myers, M. P., Wager-Smith, K., Wesley, C. S., Young, M. W. and Sehgal, A. (1995). Positional cloning and sequence analysis of the *Drosophila* clock gene, *timeless*. *Science* **270**, 805-808.

Nüsslein-Volhard, C. and Wieschaus, E. (1980). Mutations affecting segment number and polarity in *Drosophila*. *Nature* **287**, 795-801.

Pankratz, M. J. and Hoch, M. (1995). Control of epithelial morphogenesis by cell signaling and integrin molecules in the *Drosophila* foregut. *Development* **121**, 1885-1898.

Paroush, Z., Wainwright, S. M. and Ish-Horowicz, D. (1997). Torso signalling regulates terminal patterning in *Drosophila* by antagonising Groucho-mediated repression. *Development* **124**, 3827-3834.

Rauskolb, C. and Irvine, K. D. (1999). Notch-mediated segmentation and growth control of the *Drosophila* leg. *Dev. Biol.* **210**, 339-350.

Rebay, I. and Rubin, G. M. (1995). Yan functions as a general inhibitor of differentiation and is negatively regulated by activation of the Ras1/MAPK pathway. *Cell* **81**, 857-866.

Reuter, G. and Szidonya, J. (1983). Cytogenetic analysis of variegation suppressors and a dominant temperature-sensitive lethal in region 23-26 of chromosome 2L in *Drosophila melanogaster*. *Chromosoma* **88**, 277-285.

Rosenfeld, R. and Margalit, H. (1993). Zinc fingers: conserved properties that can distinguish between spurious and actual DNA-binding motifs. *J. Biomol. Struct. Dyn.* **11**, 557-570.

Rubin, G. M., Hong, L., Brokstein, P., Evans-Holm, M., Frise, E., Stapleton, M. and Harvey, D. A. (2000a). A *Drosophila* complementary DNA resource. *Science* **287**, 2222-2224.

Rubin, G. M., Yandell, M. D., Wortman, J. R., Gabor Miklos, G. L., Nelson, C. R., Hariharan, I. K., Fortini, M. E., Li, P. W., Apweiler, R., Fleischmann, W. et al. (2000b). Comparative genomics of the eukaryotes. *Science* **287**, 2204-2215.

Sambrook, J., Fritsch, E. F. and Maniatis, T. (1989). *Molecular cloning: A Laboratory Manual*. Cold Spring Harbor, NY: Cold Spring Harbor Laboratory Press.

Skaer, H. (1993). The alimentary canal. In *The Development of Drosophila melanogaster* (ed. M. Bate and A. Martinez Arias), pp. 941-1012. Cold Spring Harbor, NY: Cold Spring Harbor Laboratory Press.

So, P. L. and Danielian, P. S. (1999). Cloning and expression analysis of a mouse gene related to *Drosophila odd-skipped*. *Mech. Dev.* **84**, 157-160.

Struhl, K. (1999). Fundamentally different logic of gene regulation in eukaryotes and prokaryotes. *Cell* **98**, 1-4.

Sun, L., Liu, A. and Georgopoulos, K. (1996). Zinc finger-mediated protein interactions modulate Ikaros activity, a molecular control of lymphocyte development. *EMBO J.* **15**, 5358-5369.

Tautz, D. and Pfeifle, C. (1989). A non-radioactive *in situ* hybridization method for the localization of specific RNAs in *Drosophila* embryos reveals translational control of the segmentation gene *hunchback*. *Chromosoma* **98**, 81-85.

Tepass, U., Theres, C. and Knust, E. (1990). *crumbs* encodes an EGF-like protein expressed on apical membranes of *Drosophila* epithelial cells and required for organization of epithelia. *Cell* **61**, 787-799.

Thummel, C. S. and Pirrotta, V. (1992). Technical notes: New pCaSpeR P-element vectors. *Dros. Info. Ser.* **71**, 150.

Török, T., Tick, G., Alvarado, M. and Kiss, I. (1993). *P-lacW* insertional mutagenesis on the second chromosome of *Drosophila melanogaster*: isolation of lethals with different overgrowth phenotypes. *Genetics* **135**, 71-80.

Tsang, A. P., Visvader, J. E., Turner, C. A., Fujiwara, Y., Yu, C., Weiss, M. J., Crossley, M. and Orkin, S. H. (1997). FOG, a multitype zinc finger protein, acts as a cofactor for transcription factor GATA-1 in erythroid and megakaryocytic differentiation. *Cell* **90**, 109-119.

Venter, J. C., Adams, M. D., Myers, E. W., Li, P. W., Mural, R. J., Sutton, G. G., Smith, H. O., Yandell, M., Evans, C. A., Holt, R. A. et al. (2001). The sequence of the human genome. *Science* **291**, 1304-1351.

Waltzer, L. and Bienz, M. (1998). *Drosophila* CBP represses the transcription factor TCF to antagonize Wingless signalling. *Nature* **395**, 521-525.

Wang, L. and Coulter, D. E. (1996). *bowel*, an *odd-skipped* homolog, functions in the terminal pathway during *Drosophila* embryogenesis. *EMBO J.* **15**, 3182-3196.

Warga, R. M. and Kimmel, C. B. (1990). Cell movements during epiboly and gastrulation in zebrafish. *Development* **108**, 569-580.

Wilkins, M. R., Gasteiger, E., Bairoch, A., Sanchez, J.-C., Williams, K. L., Appel, R. D. and Hochstrasser, D. F. (1998). Protein identification and analysis tools in the ExPASy server. In *2-D Proteome Analysis Protocols* (ed. A. J. Link), pp. 531-552. New Jersey: Humana Press.

Wolfe, S. A., Nekludova, L. and Pabo, C. O. (2000). DNA recognition by Cys_2His_2 zinc finger proteins. *Annu. Rev. Biophys. Biomol. Struct.* **29**, 183-212.